Anal. Bioanal. Electrochem., Vol. 15, No. 2, 2023, 90-101
https://www.doi.org/10.22034/abec.2023.702328

Analytical & Bioanalytical Electrochemistry

Full Paper

Surface Structure and Electrochemical Behavior of Zinc-Nickel Anti-Corrosive Coating

Ramesh S. Bhat,[1,*] K. Venkatakrishna,[2] and A. Chitharanjan Hegde[2]

[1]*NITTE (Deemed to be University), NMAM Institute of Technology (NMAMIT), Department of Chemistry, Nitte-574110, India*
[2]*Electrochemistry Laboratory, Department of Chemistry, National Institute of Technology Karnataka, Srinivasnagar, 575025, India*

*Corresponding Author, Tel.: +91 8861037310
E-Mail: rameshbhat@nitte.edu.in

Received: 7 November 2022 / Received in revised form: 7 February 2023 / Accepted: 14 February 2023 / Published online: 28 February 2023

Abstract- We report on the electrodeposition of a zinc-nickel alloy using a sulphate bath on mild steel (MS) substrate. The Hull cell experiment was used to optimize the bath composition and operating conditions. Sulphanilic acid (SA) was used as an additive for the coatings. The bath demonstrated an abnormal co-deposition with more zinc being deposited over nobler nickel. The effect of temperature and current density on the coating thickness, hardness, corrosion resistance, and weight % of Ni content in the coating was investigated. The corrosion behaviour of coated zinc-nickel alloy film in sodium chloride (wt.% 3.5) solution was investigated using potentiodynamic polarization and electrochemical impedance spectroscopic approaches. The nickel content in the coatings was determined through the colorimetric method and verified by the energy dispersive X-ray spectroscopy (EDX) technique. Atomic force microscopy (AFM) and Scanning electron microscopy (SEM) techniques were used to determine the surface roughness and surface topography, of the coatings. The results show that the zinc-nickel coatings had the highest corrosion resistance (0.213 mm y^{-1}) at optimal current density (3A dm^{-2}). Thus, due to their superior corrosion resistance Zn-Ni coatings have been largely used to protect the mild steel components in many industries including the automotive, military, and aerospace segments.

Keywords- Corrosion; Electrodeposition; AFM; Hardness; XPS

1. INTRODUCTION

Electroplating of metals and alloys is widely used in many industries, with distinct advantages over other metal coating technologies [1]. The corrosion resistance of zinc coating can be enhanced by alloying with the transition group metals (such as nickel, iron, cobalt, and Mn) [2,3]. The corrosion resistance of Zinc-Nickel (ZN) alloy film depends on the wt. % of nickel in the deposit. The alloy coatings with 1-6% nickel ensure improved protection against corrosion and meet automotive industry specifications [4]. Amongst the zinc alloys, ZN alloys with varying nickel content have been the most effective for corrosion protection [5,6]. Gomez et al. [7] found that additives in the bath have upgraded the surface homogeneity and corrosion resistance even for an alloy with a small wt. % of nickel [8]. According to Ramanauskas et al. [9], the preferential dissolution of zinc at the beginning of corrosion provides good galvanic protection. As a result, the alloy becomes nickel-enriched, which increases the corrosion potential toward nobler levels and reduces the cathodic protection provided to the steel [10]. According to Shet et al. [11], the composite coatings of ZN alloy provide improved corrosion resistance by generating passive films.

As a result, there are several reports on the electrodeposition of ZN alloy done in alkaline baths such as cyanide baths or non-cyanide baths, as well as in various acidic baths including chloride baths, sulfate baths, sulfate-chloride baths, and aqueous acetate baths [12]. On the deposition of ZN alloys, numerous in-depth research projects have been published, focusing on anomalous code-position mechanisms and the dependence of deposit features on bath constitutions and operating parameters [13-16].

But no work is reported with the optimization of the ZN bath utilizing sulphanilic acid (SA) as an additional agent for the bright ZN alloy coatings. The importance of gelatin and sulphanilic acid together in the electrodeposition of ZN alloy on mild steel (MS) from a sulphate solution was identified in the current investigation. The goal of this effort is to produce the highest corrosion-resistant coatings possible by optimizing the bath compositions and cathode current densities. The coatings were characterized under ideal conditions using techniques like scanning electron microscopy (SEM), X-ray photoelectron spectroscopy (XPS), and energy-dispersive X-ray (EDX) approaches. The coating roughness was determined by Atomic force microscopy (AFM).

2. EXPERIMENTAL METHODOLOGY

2.1. Surface preparation of the substrate

The mild steel substrate with dimensions of 2.5 cm×2.5 cm (cathode) was washed with organic solvent (trichloroethylene) to remove the oil and grease. Then rust impurities were removed by using 10% sulphuric acid (pickling) and polished with emery paper of different

grit sizes (360, 500, 800, 1200, and 2000) to a flat finish. Finally, the substrates were cleaned with distilled water and dried, and used as cathodes.

2.2. Hull cell study

Merck (research grade) chemicals in distilled water were used to create electroplating solutions. The operational parameters and bath components were optimized using the Hull cell approach [17]. A Hull cell with a capacity of 267 mL was operated at 1 A cell current for 5 minutes. The cathode was made of polished MS panels, and the anode was made of pure zinc plates. Utilizing a power supply, all depositions were conducted (N6705C, Key sight Technologies). To increase the uniformity and brightness of the deposit, gelatine, and SA was combined as additives. As conducting agents for the bath and as a buffer to regulate the pH of the bath, ammonium chloride and potassium chloride were utilized. Each component can vary, and deposit patterns were scrutinized for how they appeared. Based on how the coatings appear, the bath composition and CD have been improved. Over a broad CD range of 1.0-5.0 A dm^{-2}, deposits with a porous solid/bright/semi-bright /greyish-white appearance were produced. Based on the bath compositions, the uniformity of coating film, and optimization parameters are given in Table 1. For comparison, all depositions were performed galvanostatically for 10 minutes at lab temperature with a pH of 3.

Table 1 Composition of the electroplating bath and operation conditions

Bath composition	Amount (g/L)	Operating conditions
$ZnSO_4$	105.0	pH: 3.0
$NiSO_4.6H_2O$	90.0	Temperature: 30 °C
NH_4Cl	100.0	Anode: Pure Zn
KCl	120.0	CD: 3.0 A dm^{-2}
Sulphanilic acid	5.0	
Gelatine (gL^{-1})	5.0	

2.3. Corrosion analysis

The corrosion behavior of the coatings was assessed by polarization and electrochemical impedance spectroscopy (EIS) methods. All electrochemical experiments were performed using a three-electrode cell and a potentiostat (CH instrument-604E). The counter was a platinum electrode, and the working was a coated specimen. The calomel electrode was used to identify all electrochemical potentials mentioned in this work (SCE). The corrosive media for the investigation was a 3.5 wt.% NaCl solution. At a scan rate of 0.01 mVs^{-1}, potentiodynamic polarization investigation was conducted in a potential ramp of ±0.20V

around open circuit potential (OCP). The Tafel extrapolation technique was used to calculate the corrosion rates. The impedance measurements were performed using sine waves with an amplitude of 10 mV throughout a frequency range of 100 KHz to 1 MHz. A cyclic polarization investigation in the potential range of -0.5V to 1.0V was used to further analyze the nature of corrosion.

2.4. Surface analysis

SEM was used to evaluate the microstructure of the deposits (JSM-6380, Japan). Using a digital thickness tester, the thickness of the deposits was confirmed after being computed using Faraday's law. The colorimetric approach was used to determine the wt.% of nickel in the coating [17]. Using a Micro Hardness Tester, the Vickers method was used to determine the hardness of the coatings (20 m in thickness). Knowing the bulk and composition of the coating allowed one to calculate the cathode current efficiency (C.C.E.) of the deposition [18]. Atomic Force Microscopy (AFM, PicoSPM^{TM} from Molecular Imaging) and X-ray Photoelectron Spectroscopy 5600 Multi-Technique System are used for surface analysis (PHI, USA).

3. RESULTS AND DISCUSSION

3.1. Effect of current density

The ZN films have been prepared onto the MS using direct current from the optimal bath. The alloy coating, the CD has a major role in the coating composition, structure, and properties. This alloy bath produced semi-bright deposits at low CD. and porous bright deposits at high CD. A sound deposit was found at optimized CD (3.0 A dm^{-2}) with 3.90 wt.% nickel was achieved. The effects of applied CD on the C.C.E, and the chemical composition of the alloys are shown in Figure 1. The mass of the deposit gained in each CD is determined, and from which the concentration of Ni is found by the colorimetric method and is listed in Table 2. In all cases, the C.C.E was very high (viz. higher than 90%) [19,20]. In general, a small decrease in C.C.E with increasing CD was observed, which may be due to too much hydrogen evolution on the cathode (Figure 1).

Table 2. Impact of CD on the wt. % nickel, and mechanical properties of ZN coatings

i (A dm^{-2})	wt.% nickel	VHN	Thickness µm	$-E_{corr}$ ($V_{vs.}$ SCE)	i_{corr} (µA cm^{-2})	CR (mm y^{-1})
1.0	6.03	171	10.7	1.062	39.44	0.546
2.0	3.41	198	15.7	1.081	31.59	0.450
3.0	3.90	219	20.3	1.141	14.81	0.212
4.0	5.47	212	25.1	1.116	17.78	0.258
5.0	9.90	202	27.6	1.088	36.28	0.564

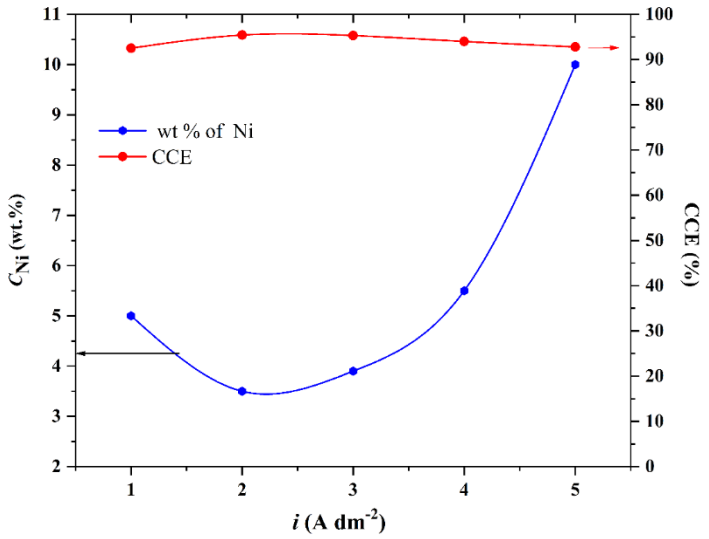

Figure 1. Cathode current efficiency and the wt.% of nickel in the deposit at different CD

3.2. Effect of pH and temperature

In ZN deposition, the pH has little effect on deposition from baths, containing simple metal ions. The variation in the wt.% nickel in the deposit with pH and temperature, at optimum CD, i=3.0 A dm^{-2} is shown in Figure 2. The increase of nickel content with pH indicates that the metal ions are in complex form. Bath temperature has a significant role in the composition and appearance as exhibited by other Zn-Fe group metal alloys. The bath temperature was varied from 10 ºC to 50 ºC. The wt. % nickel in the deposit was found to be decreased with temperature (Figure 2). This is due to the rapid depletion of cathode film, which resulted in the deposition of zinc-rich, as observed in anomalous co-deposition of Zn-Fe group alloys [1].

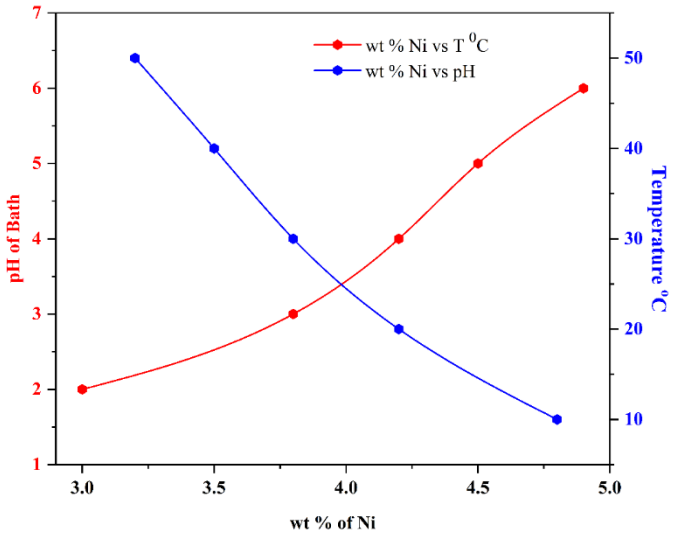

Figure 2. Effect of pH and temperature on the wt. % of Ni in the deposit at CD, i=3.0 A dm^{-2}

3.3. Thickness and Hardness of deposit

As the applied CD increased, the thickness of the all-alloy coating also increased, as indicated in Table 2. The increase in thickness may be attributed to the sealing of metal hydroxides in the crystal lattices, due to a limited increase in pH, caused by excessive hydrogen evolution. On the other hand, the Vickers hardness increased with CD to a maximum value and then decreased at higher CD (Table 2). The highest hardness was observed at optimum CD (i=4.0 A dm^{-2}), then decreased at higher CD.

3.4. Tafel extrapolation method:

The corrosion behavior of the alloy coatings was studied by electrochemical methods in sulphate solution, and corresponding data are summarized in Table 2. Potentiodynamic polarization curves of ZN alloy deposits (only representative) are shown in Figure 3.

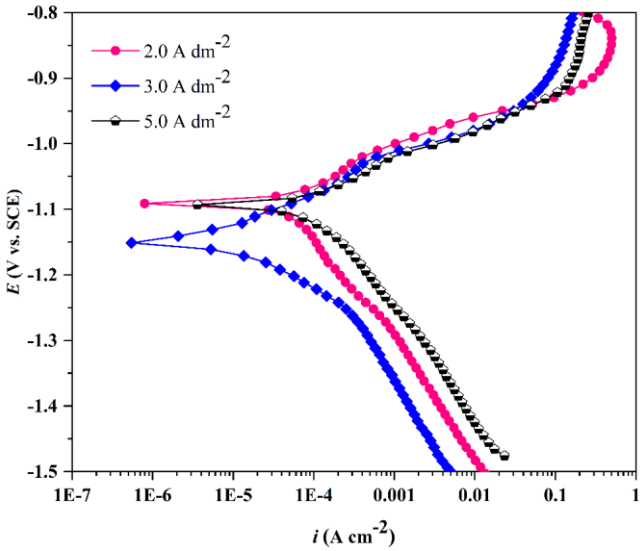

Figure 3. Polarization curves of ZN coatings

The least corrosion rate (0.212 mm y^{-1}) was observed for the deposit obtained at i = 3.0 A dm^{-2}. From Table 2, it is evident that the least possible corrosion rate corresponds to neither high nickel content nor thickness of the coating. Less corrosion rate at optimal CD may be attributed to better dissolution of zinc, leaving the upper layer enriched with nickel, which acts as a barrier for further attack, as envisaged by many workers [22]. The mechanism of corrosion during the reaction was studied using the cyclic polarisation method. The polarization curves show that localized corrosion starts and continues at the corrosion potentials coating. The potential is swept once, and the amount of hysteresis and the variations in the initial open circuit corrosion potential and return passivation potential values are also investigated [23]. Pitting corrosion is indicated by the hysteresis in Figure 4, and the amount of pitting corrosion in the electroplated ZN alloy correlates with the size of the loop.

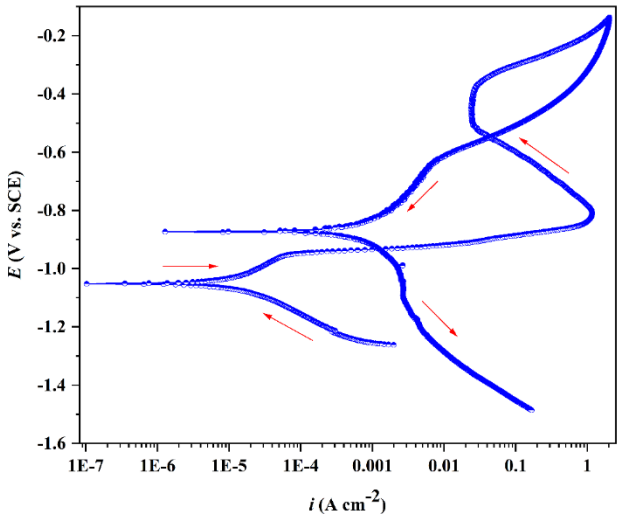

Figure 4. Cyclic polarization curves of ZN coating at 3.0 A cm^{-2}

3.5. Electrochemical Impedance Spectroscopy (EIS) method

EIS was utilized to assess the polarization resistance of the coatings and barrier qualities. Figure 5 displays the Nyquist response of ZN alloy deposits at various CDs. Given that the same bath chemistry and cell layout were applied in each example, it should be noted that the solution resistance Rs is essentially the same in all of them. However, as the applied CD rose, polarization resistance, or R_P, increased. It is possible to see that the radii of capacitive loops rise with a CD up to 3.0 A dm^{-2} and subsequently decreased, which is consistent with the outcomes of Tafel's approach. The deposit is the most corrosion-resistant with the highest Rp value, according to the capacitive loop with the largest diameter, which corresponds to the coating at best CD (3.0 A dm^{-2}). But for deposits at higher CD. (At 4.0 and 5.0 A dm^{-2}), the radii of the semi-circle decreased extremely, as shown in Figure 5, indicating their poor corrosion resistance.

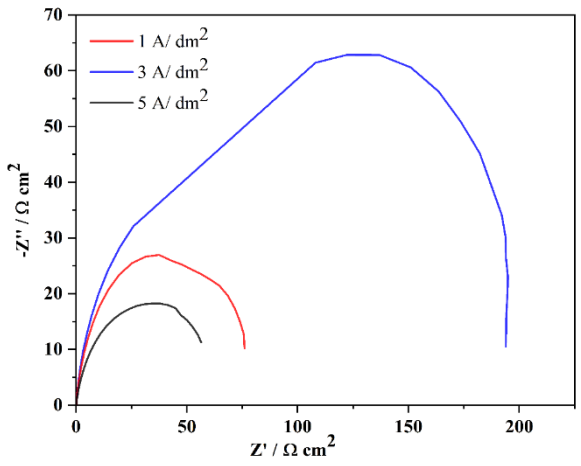

Figure 5. Nyquist plots of ZN alloy coatings (only representative) at various CDs

It should be noted that for the proposed equivalent circuit made up of solution resistance, Rs, polarization resistance, R_P, and double layer capacitance, C_{dl}. Nyquist plots for ZN electroplated alloys do not form perfect semicircles as predicted by the EIS theory. The reason for such deviation may be explained as follows: The electrified interface between the substrate and medium does not fit into a real capacitor. The charge distribution is governed by ions on the solution side while electrons govern it on the metal side. Because ions are significantly larger than electrons, they will take up a significant amount of space on the solution side of the double layer [24,25].

3.6. Surface chemistry

The surface plays a crucial role, for instance in microelectronics, catalysis, corrosion, etc., as the medium via which the solid interacts with its environment [26]. While studying the surface properties, one is interested in its structure and chemical composition that is, the chemical bonding at the surface and in the surface layer. Yet, one does not restrict oneself to the uppermost layer only. It is important to examine further layers, even to a depth of a few nanometers thick, because properties related to the surface are also influenced by the subsurface layers. Among different techniques for studying surface properties, X-ray photoelectron spectroscopy (XPS) is also one and is employed in the present study. Figure 6 displays the XPS spectra of coating before and after sputter cleaning.

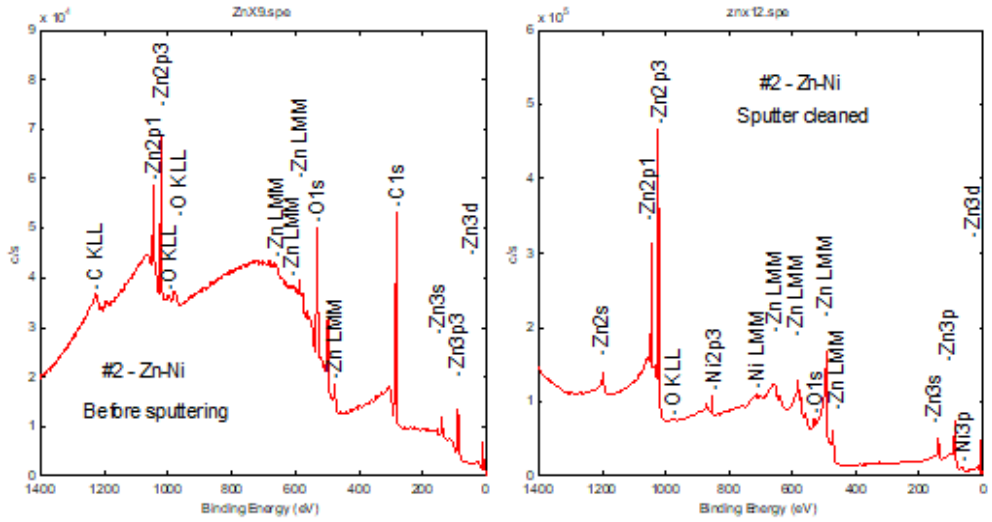

Figure 6. XPS spectra of ZN alloy deposit at 3.0 A dm $^{-2}$ before, and after sputtering

The Z2p3/2 spectrum of zinc (Z) ($L_3M_{45}M_{45}$) was shown in Figure 7 since it is challenging to distinguish between non-oxidized zinc (Z) and oxidized zinc (ZO) since the spectra are identical for both states (1020.6 eV and 1020.7 eV). After sputter cleaning, the chemical compositions are reported. The ZN alloy had just C, O, Z, and N (in descending sequence)

visible at the surface before sputtering. According to Figure 7, Z is present in the bulk of the material in the non-oxidized (Z) state, but it is also present in the oxidized (ZO) state at the surface of the ZN coating just before sputtering. The nickel was revealed in the outer layer in the non-oxidized form, while zinc was in the oxidized form, as indicated by the electron energy peaks. The energy peak at 992 eV indicates that zinc oxide does indeed appear at deeper depths. Within the concentration profile under study, nickel was found to be non-oxidized. As a result, less noble zinc corrodes faster than more noble ones like nickel, which doesn't corrode [27].

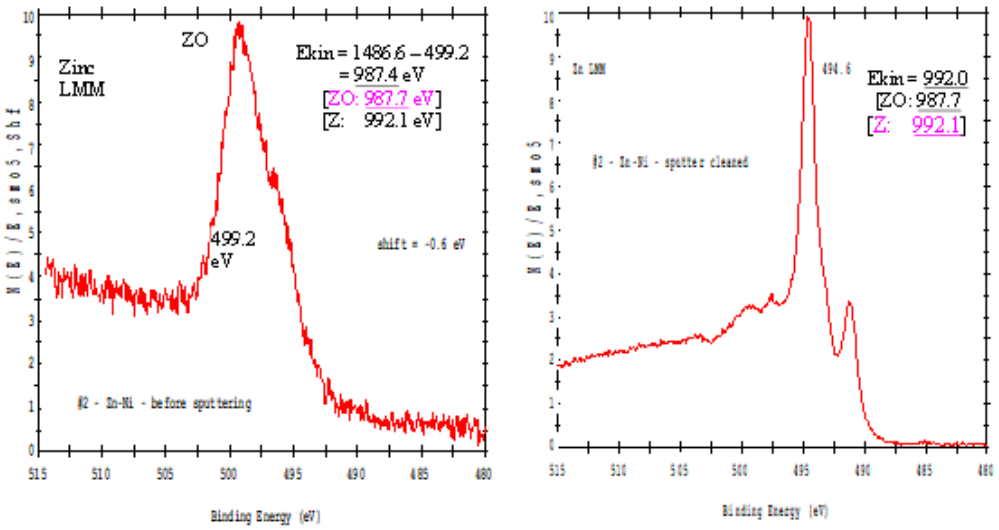

Figure 7. XPS spectra showing Z_{LMM} peak of ZN alloy deposit before and after sputtering.

The 2D AFM images of the ZN deposit, at optimized processing parameters, are shown in Figure 8. Using the PicoSPM^{TM} software, the mean roughness Ra, and root-mean-square roughness Zrms, were calculated from AFM images. For electrodeposited ZN coating, the Ra and Zrms values were revealed to be 34.5 nm and 41.2 nm, respectively.

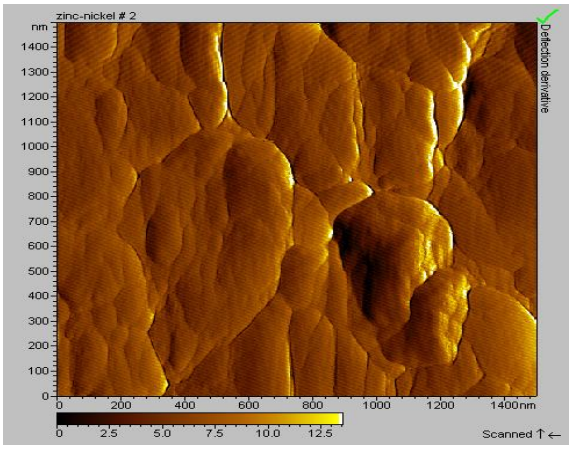

Figure 8. 2D AFM image of ZN alloy deposit at CD=3.0 A dm^{-2}

The SEM image in Figure 9 (a-c) shows the surface morphologies of ZN coatings at different CDs. In low CD, the coating was very thin and grayish (a), at higher CD, the deposit was thick and burnt with porous(c). At optimum CD, the deposit was uniform, bright, and without any cracks (b).

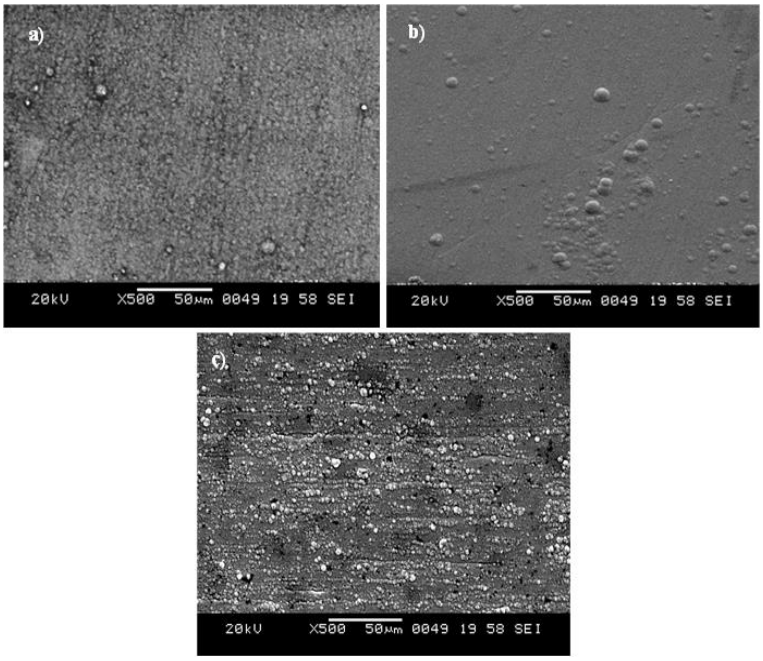

Figure 9. Surface morphology of ZN alloy coatings at different current densities (a) 1.0 A dm^2, (b) 3.0 A dm^{-2} (c) 5.0 A dm^{-2}

EDX analysis (3.0 A dm^{-2}) confirms the presence of carbon (9.05%), oxygen (7.28 %), nickel (3.20), and zinc (81.47%) present in the coating. The wt.% of nickel from EDX is approximately in agreement with that obtained by the colorimetric method as shown in Table 2. The deviation, in the wt. % nickel by the EDX method may be due to the randomness in the detector counts caused by the roughness of the coated surface.

4. CONCLUSION

The MS substrate was electroplated with ZN alloy using a sulphate bath with sulphanilic acid (SA) as an additive. The composition, hardness, and thickness of the coatings were examined in relation to the applied CD, and pH. The cathode current efficiency of the bath under different conditions of temperature was studied. The polarization and EIS study revealed that the ZN coatings obtained at i=3.0 A dm^{-2}, having 3.9 wt. % Ni content and have the highest corrosion resistance compared with other current densities. According to an XPS investigation, the more noble nickel does not corrode while the less noble zinc corrodes during the initial phases of corrosion. The dendritic growth of the coatings under different CDs as examined by the SEM indicated that the electro-crystallization process is mass transport-controlled. The

corrosion performance of the ZN coating is dependent on neither the wt. % Ni nor the thickness of the deposit. It also signifies that the ZN alloy has the potential application in automobile and defense applications.

Declarations of interest

The authors declared that they have no conflict of interest.

REFERENCES

[1] A. Brenner, Electrodeposition of Alloys. Vol. 2, Academic Press, New York 194 (1963).
[2] G. Barcelo, E. Garcia, M. Sarret, and C. Muèller, J. Appl. Electrochem. 28 (1998)1113.
[3] P. P. Chung, J. Wang, Y. Durandet, Friction 7 (2019) 389.
[4] R. S. Bhat, K. B. Munjunatha, S. I. Bhat, K. Venkatakrishna K, and A. C. Hegde, J. Mater. Eng. Perform. (2022) 1.
[5] V. Thangaraj, and A. C. Hegde, Bull. Electrochem. 22(2) (2006) 49.
[6] J. B. Bajat, M. D. Maksimovi, and G. R. Radovi, J. Serb. Chem. Soc. 67 (2002) 625.
[7] E. Gomez, X. Alcobe, and E. Valles, J. Electroanal. Chem. 505 (2001) 54.
[8] R. S. Bhat, K, B, Manjunatha, R, Prasanna Shankara, K. Venkatakrishna, and A. C. Hegde, Applied Physics A 126 (2020) 772.
[9] R. Ramanauskas, P. Quintana, L. Maldonado, R. Pomes, and M. A. Pech-Cnul, Surf. Coat. Technol. 92(1997) 16.
[10] M. M. Abou-krisha, A. M. Zaky, and A. A. Toghan, J. Corros. Sci. Eng. 7(2005) 19.
[11] V. B. Shet, R. S. Bhat, R. Selvaraj, Guru Prasad, A. Kodgi, A. Damodaran, and A. Savithri, Appl. Nanosci. 11 (2021) 2469.
[12] W. Yun-yan, X. Hai-juan, and C. Li-yuan. J. Cent. South Univ. Technol. 15 (2008) 814.
[13] R. S. Bhat, S. Bekal, and A. C. Hegde, Anal. Bioanal. Electrochem. 10 (2018) 1562.
[14] R. S. Bhat, and A. C. Hegde, Transactions of the IMF 93 (2015) 157.
[15] R. S. Bhat, K. Venkatakrishna, J. Nayak, and A. C. Hegde, J. Mater. Eng. Perform. 29, (2020) 6363.
[16] R. S. Bhat, Fabrication of Multi-Layered Zn-Fe Alloy Coatings for Better Corrosion Performance, Liquid Metals, Intech Open publisher (2021).
[17] N. Kanani, Electroplating-Basic Principles, Processes, and Practice, Elsevier Pub. Ltd. UK (2006).
[18] V. Thangaraj, and A. C. Hegde, Bull. Electrochem. 22 (2006) 49.
[19] R. S. Bhat, P. Nagaraj, and S. Priyadarshini, Surf. Eng. 37 (2021) 755.
[20] R. S. Bhat, and A. C. Hegde, Anal. Bioanal. Electrochem. 6 (2014) 606.
[21] R. S. Bhat, and A. C. Hegde, Anal. Bioanal. Electrochem. 4 (2012) 593
[22] N. Koura, Y. Suzuki, Y. Idemoto, T. Kato, and F. Matsumoto, Surf. Coat. Technol. 169 (2003) 120.

[23] A. Kocijan, and M. Jenko, Mater. Technol. 40 (2006) 1.
[24] E. Laouini, M. Hamdani, M. I. S. Pereira, J. Douch, M. H. Mendonc¸ Y. Berghoute, and R. N. Singh, J. Appl. Electrochem. 38 (2008) 1485.
[25] M. E. Orazem, and B. Tribollet, Electrochemical impedance spectroscopy. Wiley & Sons, Inc., Hoboken, New Jersey (2008).
[26] S. Amelinckx, Drik van Dyck, J. van Landuyt, and Gustaaf van Tendeloo, Handbook of Microscopy-Applications in Materials Science, Solid-state Physics and Chemistry, Vol 3, Wiley-VCH (1997).
[27] S. Lichusina, A. Chodosovskaja, A. Sudavicius, R. Juskėnas, D. Bucinskienė, A. Selskis, and E. Juzeliunas, Chemija 19 (2008) 25.